

Bimetallic nano and micro alloys of transition metals $\text{Co}_x\text{Ni}_{(1-x)}$

F. Barffuson-Dominguez¹, R. Gámez-Corrales¹, J. R. González-Martínez², O. Alcantar-Jatomea³
G.T. Paredes-Quijada⁴

¹F. Barffuson-Domínguez, Departamento de Física, Universidad de Sonora, Apdo. Postal 1626, 83000, Hermosillo, Sonora, México.

¹R. Gámez-Corrales, Professor, Departamento de Física, Universidad de Sonora, Apdo. Postal 1626, 83000, Hermosillo, Sonora, México. E-mail: rogelio.gamez@unison.mx.

²J.R. González-Martínez, Departamento de Investigación en Física, Universidad de Sonora, Apdo. Postal 1626, 83000, Hermosillo, Sonora, México.

³O. Alcantar-Jatomea, Departamento de Ciencias Básicas, Tecnológico Nacional de México, campus Hermosillo, 83170, Hermosillo, Sonora, México.

⁴G.T Paredes-Quijada, Departamento de Ciencias Químico-Biológicas, Universidad de Sonora, 83000, Hermosillo, Sonora, México.

Abstract – Bimetallic nanoalloys of transition metals represent a field of considerable potential, and research endeavors in this domain are of significant interest. These intriguing materials have garnered substantial interest due to their numerous applications as catalysts for hydrogen and Fischer-Tropsch synthesis, magnetic fluids, and magnetic data storage. Additionally, their biomedical applications include drug delivery and cancer treatment through hyperthermia. In this pioneering study, we delve into the intricacies of the fabrication and nanostructures of $\text{Co}_x\text{Ni}_{(1-x)}$ nanoalloys. In the fabrication process of these bimetallic nanoalloys, high-energy micromechanical milling was employed to produce soft transition metals. These metals were produced using powdered cobalt and nickel in varying ratios. Subsequently, a scanning electron microscope (SEM) was employed to obtain a more detailed view of the nanostructures of the nanoalloys. The SEM data revealed hierarchical patterns of spherical formations with nanometric sizes down to 10 microns.

Key Words: SEM, micromechanical milling, $\text{Co}_x\text{Ni}_{(1-x)}$, nano-alloys, hierarchical structures.

1. INTRODUCTION

In recent years, nanostructured alloys have garnered heightened interest due to the potential for precise control over their size and shape while retaining the distinct properties of each constituent metal. These properties render them suitable for diverse industrial and scientific applications. Transition metals have been the subject of numerous applications, particularly for biomedicine, where bimetallic nanoalloys have been utilized in magnetic hyperthermia treatments for cancer. These nanoalloys augment local heat, leading to the destruction of cancerous cells. The potential of bimetallic nanoalloys extends to various fields, including drug delivery, magnetic resonance imaging (MRI), cell separation, biomarker detection, and bacterial infection treatment. Another area of application is catalysis, where bimetallic nanoparticles have found

widespread use in hydrogenation reactions, including the reduction of nitrophenols and the hydrogenation of biomass-derived compounds such as levulinic acid and glycerol, and Fischer-Tropsch synthesis, magnetic fluids, and magnetic data storage. The development of a myriad of applications of this type of bimetallic nanomaterial can be attributed to its morphology. These include chains of spheres [1], columnar structures [2], polydisperse quasi-spherical nanoalloys of various sizes [3], quasi-spherical micrometric alloys [4], starfish-type [5], nanoflakes [6], micrometric flowers formed by sequin-type structures [7]. Shell-core nanoparticles [8], Mushroom-type microstructures [9], nanofibers, metal alloy nanotubes, hollow spheres [10], nanocrystals [11], and nanowires [12], among others, have also been identified.

This study investigated the morphology of $\text{Co}_x\text{Ni}_{(1-x)}$ nanoalloys using inverted optical and scanning electron microscopy. The high-energy mechanical milling technique was selected for its cost-effectiveness and ease of control over the structures to be obtained.

2. EXPERIMENTAL DETAILS

2.1 Sample preparations

The cobalt and nickel materials were obtained from Sigma-Aldrich in powder form, with a purity of 99% for cobalt and 99% for nickel, and were used without prior purification treatment. The average powder size indicated by Sigma Aldrich for cobalt and nickel was less than 10 and 50 micrometers, respectively. The nanometric particles (alloys) were obtained by the high-energy mechanical grinding method using high-energy Fritsch Pulverisette 5 and 6 planetary mills (Figure 1). In all the samples in this study, the cobalt-nickel ratio was systematically varied, considering its established stoichiometries: $\text{Co}_x\text{Ni}_{(1-x)}$ [$x=0.9, 0.7, 0.5, 0.3, 0.1$]. The grinding was performed for each sample of nanoalloy nanostructures for 24 hours at 350 RPM with 6 mm and 8 mm diameter steel balls in agate containers of 65

ml capacity. The grinding was executed at a mass ratio of balls to powder mass of 20:1, with 3 grams of the sample utilized for each synthesis.



Figure 1: Fritsch Pulverisette 5 and 6 high-energy planetary mills, each equipped with a 65 ml bowl.

2.2 Optical and Scanning Electron Microscopy

Optical micrographs were obtained using a LABOMEX model MET 400 metallurgical optical microscopes with a 100X objective while scanning electron microscopy (SEM) micrographs were obtained using a JEOL model JSM-7800F microscope. Energy dispersive spectroscopy measurements were carried out using a Bruker XFlash 6-60 detector.

3. RESULTS AND DISCUSSION

As illustrated in Figure 1, the Fritsch Pulverisette 6 planetary mill, equipped with a 65-ml bowl functioning as a high-energy reactor, has been utilized in the experimental setup. These high-energy mills, while effectively reducing the size of the powder components of the reactants (Co and Ni), have been shown to generate sufficient thermal energy to form or aggregate two or more elements, forming alloys and quasi-stable structures.

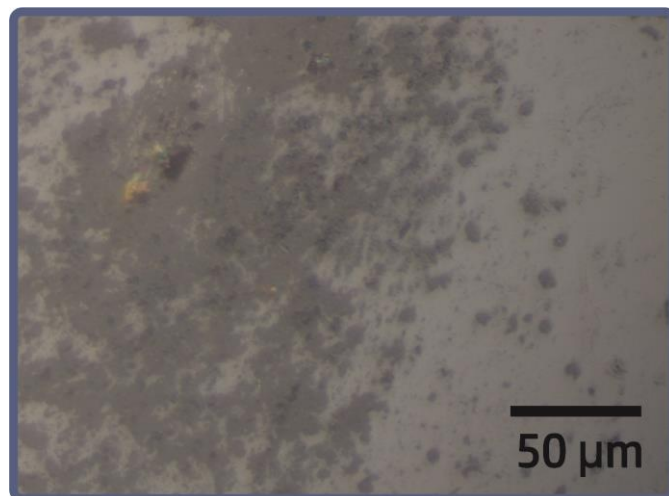


Figure 2: A micrograph was obtained using optical microscopy at 200x magnification of the $\text{Co}_x\text{Ni}_{(1-x)}$ alloy, with x set at 0.9.

Morphological characterizations of $\text{Co}_x\text{Ni}_{(1-x)}$ nanoalloys were carried out using two experimental techniques: optical microscopy (OM) and scanning electron microscopy (SEM). The image obtained from optical microscopy reveals the presence of aggregates in a representative sample of a $\text{Co}_{0.9}\text{Ni}_{0.1}$ alloy, with a composition of 90% Co and 10% Ni (Figure 2). The sample displays polydispersity in the size distribution of the aggregates, with sizes ranging from a few hundred nanometers to tens of microns.

The morphology obtained in SEM is shown in Figure 3. In this figure, Co-Ni alloys with a ratio of 70:30 can be observed (Figure 3A), and Figure 3b corresponds to the chemical composition NiCo 70:30. The following presentation provides an in-depth comparative analysis of two SEM images of Co-Ni alloys. The present study considers the micrographs identified as CoNi 70-30 and NiCo 70-30. The lower white bar of each image, corresponding to 1 μm , is used to estimate the dimension and nanometer scale in both samples. The micrograph shows particles with well-defined contours, ideally spherical or slightly oval. The uniformity in morphology suggests precise control in the synthesis process, emphasizing homogeneous nucleation and well-defined growth.

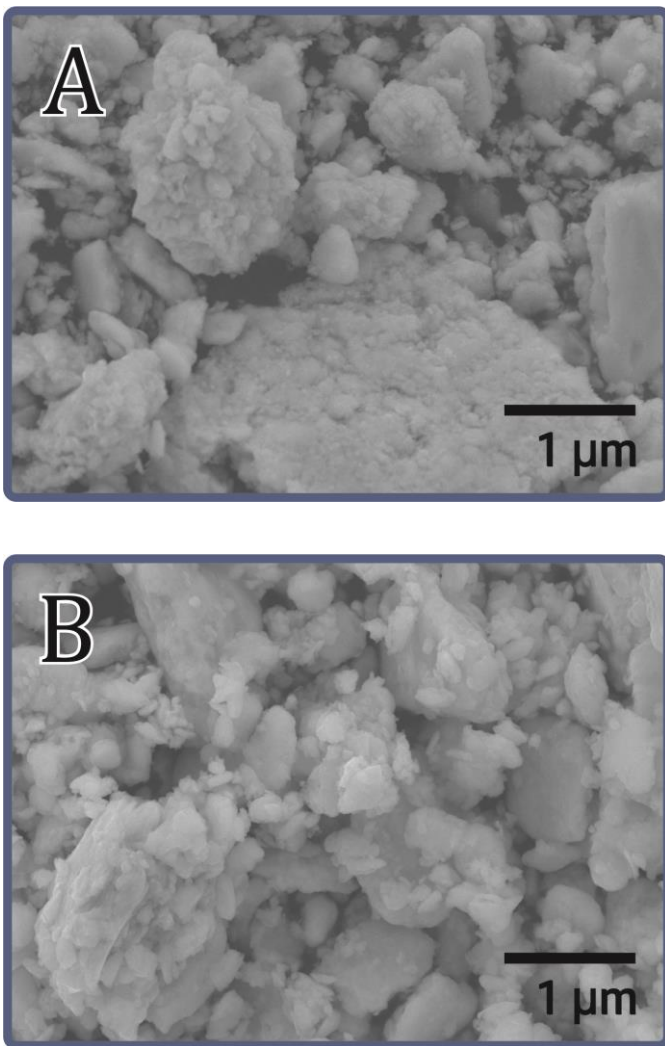


Figure 3: A. SEM CoNi 70-30. B. SEM NiCo 70-30.

As illustrated in Figure 3A, the hierarchical structures of amorphous form and sizes of a dozen microns are evident. These structures are constituted by lamellar structures with a thickness of several tens of nanometers and a size comparable to the amorphous microparticles, as depicted in Figure 3A, which was obtained under a magnification of 5,000X. This figure reveals the presence of amorphous microstructures, with the largest measuring approximately 10 microns. This magnification level facilitates the observation of internal details. The lamellar structures under scrutiny consist of lamellar aggregates measuring several hundred nanometers.

Conversely, as demonstrated in Figure 3B (NiCo 70%-30%), the image unveils a more irregular morphology, with particles displaying a propensity to form agglomerates or even branched structures. The distribution in this sample deviates from the previous one in that it lacks uniformity; regions exhibiting higher particle density and those characterized by interparticle voids are discernible. Utilizing

the same reference of 1 μm from the scale bar, it is estimated that the particles possess a larger average diameter or, in certain instances, a greater dispersion in their dimensions, with a range of 150 to 400 nm. The observed size variability indicates less uniform growth processes and a heightened tendency toward partial coalescence.

Observation of areas featuring augmented porosity, in conjunction with the aggregation of nanoparticles exhibiting a cushioned consistency, suggests that the growth mechanism may have been impacted by multi-centered nucleation and anisotropic growth. Evidence has demonstrated that this may augment the size of the active surface area. In certain applications, such as catalysis, this increase is advantageous.

The ensuing discourse presents a thoroughgoing analysis and comparison of the two SEM micrographs incorporated within the present document, assuming that said micrographs correspond to images of the CoNi-50 (see Figure 4A) material exhibiting variations in its nanometer-scale structural configuration. Figure 4A displays a more homogeneous and compact nanometric structure. The nanoparticles under scrutiny manifest as spherical or slightly oval-shaped entities, characterized by well-defined edges and a consistent distribution along the surface. The uniformity in size and compactness of the nanomaterials suggests that its growth occurred under controlled conditions that promoted the formation of a single nanocrystalline phase, with an estimated particle size ranging from 20 to 50 nanometers. The low porosity and bulk density of nanoparticles indicate a nucleation and growth process without significant coalescences, which is advantageous when uniform magnetic or electronic properties are desired.

In contrast, Figure 4B displays a more heterogeneous and branched structure. Agglomerates and dendritic structures can be identified in areas where nanoparticles are grouped. These agglomerates manifest a greater dispersion in size, with estimated sizes ranging from approximately 40 to 80 nanometers, although some substructures appear to exceed these values. The presence of regions with obvious voids or interparticle pores suggests that growth was dominated by partial coalescence and crystal reorientation phenomena. These phenomena may influence properties such as catalytic response or surface activity. This type of less ordered morphology could be associated with different synthetic conditions or post-synthesis treatment that favored the formation of multiple phases or structural defects.

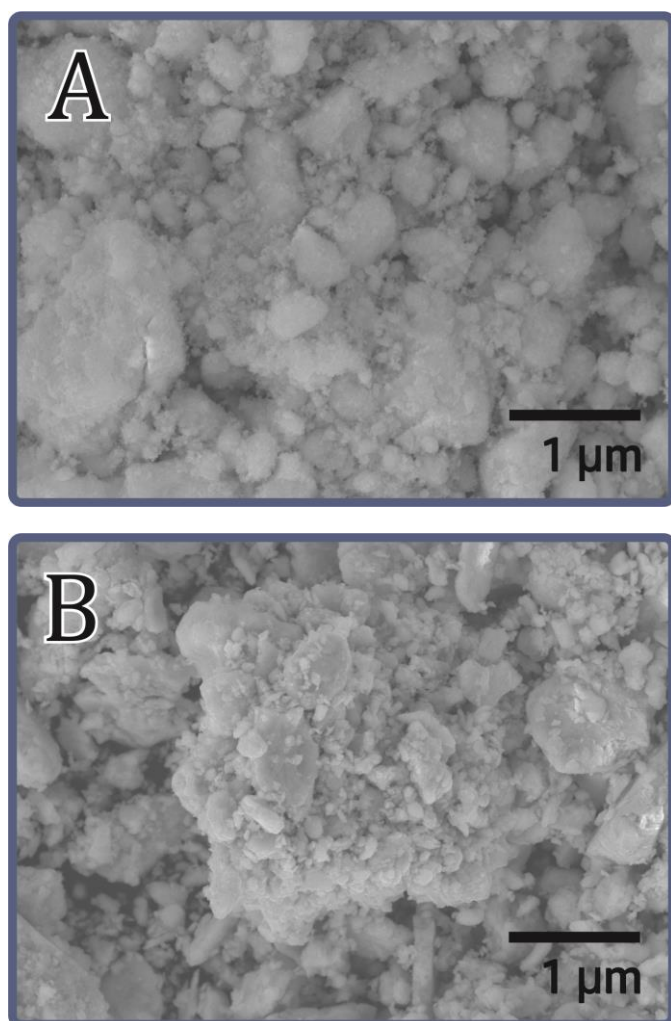


Figure 4. A. SEM CoNi 50-50. **B.** SEM NiCo 50-50.

The contrast between the two images indicates that the synthesis conditions or post-synthesis treatment significantly influenced the nucleation and growth process of the CoNi 50%-50% material. Figure 4A which exhibits a homogeneous structure and compact nanoparticles, suggests controlled and potentially single-phase growth, a property that is advantageous for achieving uniform magnetic characteristics. Figure 4B demonstrates a more intricate morphological evolution characterized by agglomerates and elevated porosity, which may yield divergent functionalities, particularly in applications where surface-substrate interaction or catalytic activity are pertinent.

4. CONCLUSIONS

This work constitutes an experimental study, utilizing optical microscopy (OM) and scanning electron microscopy (SEM), which was conducted on bimetallic alloys comprised of transition metals, namely cobalt and nickel. The synthesis was performed with micromechanical milling at a Cox-Ni1-x ratio of x (= 90, 70, 50, 30, 10) and a pellet/material ratio of 20 to 1. As demonstrated by optical microscopy, the samples

exhibited heterogeneity, accompanied by polydisperse structures with dimensions ranging from tens of nanometers to several tens of micrometers. The scanning electron microscope (SEM) reveals micro images of quasi-spherical nanoparticles of bimetallic alloys, with a size ranging from 40 to 50 nanometers. These nanoparticles self-assemble into lamellar structures, with a thickness corresponding to the diameter of the quasi-nanospheres. Due to the substantial amount of thermal energy provided by mechanical milling, the lamellar structures self-assemble to form hierarchical structures with larger sizes (approximately ten microns in diameter) and amorphous shapes, different from their constituents.

REFERENCES

- [1] G. Cheng, "Fabrication and characterization of iron-nickel chain-like fibers via simple solvothermal approach," *Mater. Res. Innov.*, vol. 19, no. 1, pp. 69–72, 2015, doi: 10.1179/1433075X14Y.0000000222.
- [2] G. Dhanalakshmi and V. Ravichandran, "Synthesis of nanocrystalline nickel-iron alloys-A novel chemical reduction method," *Chem. Phys. Impact*, vol. 6, no. March, p. 100202, 2023, doi: 10.1016/j.chphi.2023.100202.
- [3] L. Li *et al.*, "High valence metals engineering strategies of Fe/Co/Ni-based catalysts for boosted OER electrocatalysis," *J. Energy Chem.*, vol. 76, pp. 195–213, 2023, doi: 10.1016/j.jechem.2022.09.022.
- [4] I. Chicinas, V. Pop, and O. Isnard, "Synthesis of the superalloy powders by mechanical alloying," *J. Mater. Sci.*, vol. 39, no. 16–17, pp. 5305–5309, 2004, doi: 10.1023/B:JMSc.0000039234.58490.78.
- [5] N. Nady, N. Salem, M. A. A. Mohamed, and S. H. Kandil, "Iron-nickel alloy with starfish-like shape and its unique magnetic properties: Effect of reaction volume and metal concentration on the synthesized alloy," *Nanomaterials*, vol. 11, no. 11, 2021, doi: 10.3390/nano11113034.
- [6] W. Kang, "Microforging Effect on the Microstructure and Magnetic Properties of FeSiB-based Nanoflakes," *J. Mater. Sci. Technol.*, vol. 28, no. 4, pp. 303–307, 2012, doi: 10.1016/S1005-0302(12)60058-9.
- [7] L. Liu, J. Guan, W. Shi, Z. Sun, and J. Zhao, "Facile synthesis and growth mechanism of flowerlike Ni-Fe alloy nanostructures," *J. Phys. Chem. C*, vol. 114, no. 32, pp. 13565–13570, 2010, doi: 10.1021/jp104212v.
- [8] Y. Zhang, C. Liu, G. Fan, L. Yang, and F. Li, "A robust core-shell nanostructured nickel-iron alloy@nitrogen-containing carbon catalyst for the

- highly efficient hydrogenation of nitroarenes," *Dalt. Trans.*, vol. 47, no. 38, pp. 13668–13679, 2018, doi: 10.1039/c8dt03033b.
- [9] T. Han, C. Xu, and H. Chen, "Simple synthesis of novel mushroom-like FeNi₃ microstructures by a hydrothermal reduction," *Mater. Res. Innov.*, vol. 23, no. 1, pp. 39–42, 2017, doi: 10.1080/14328917.2017.1362509.
- [10] G. Tong, J. Guan, Z. Xiao, F. Mou, W. Wang, and G. Yan, "In situ generated H₂ bubble-engaged assembly: A one approach for shape-controlled growth of Fe nanostructures," *Chem. Mater.*, vol. 20, no. 10, pp. 3535–3539, 2008, doi: 10.1021/cm800269k.
- [11] F. Ebrahimi and H. Q. Li, "Structure and properties of electrodeposited nanocrystalline FCC Ni-Fe alloys," *Rev. Adv. Mater. Sci.*, vol. 5, no. 2, pp. 134–138, 2003.
- [12] M. Zeng, H. Yang, J. Liu, and R. Yu, "Gradient magnetic binary alloy nanowire," *J. Appl. Phys.*, vol. 115, no. 17, pp. 113–116, 2014, doi: 10.1063/1.4864248.